J. Electrochem. Sci. Eng. **16** (2026) 3157; https://doi.org/10.5599/jese.3157

Open Access : : ISSN 1847-9286

https://pub.iapchem.org/ojs/index.php/JESE

Original scientific paper

Poly(asparagine)-modified duplex stainless steel composite carbon paste electrode for selective electrochemical detection of dopamine

Shashanka Rajendrachari[1,✉], Hareesha Nagarajappa[2], Varun Donnakatte Neelalochana[3], Rakshitha Gattavadipura Shivaraju[4], Ersin Demir[5], Santhy Antherjanam[6], Kazim Erden Karaoglanli[7]

[1]*Department of Chemistry, Global Academy of Technology, Bangalore-560098, Karnataka, India*
[2]*Department of Chemistry, Soonchunhyang University, Asan 31538, Republic of Korea*
[3]*Department of Civil, Environmental and Mechanical Engineering, University of Trento, Via Mesiano, 77, Trento 38123, Italy*
[4]*Department of Chemistry, SJCE, JSS Science and Technology University, Mysuru-570 006, Karnataka, India*
[5]*Department of Analytical Chemistry, Faculty of Pharmacy, Afyonkarahisar Health Sciences University, Afyonkarahisar 03100, Türkiye*
[6]*Department of Chemistry, Amrita Vishwa Vidyapeetham, Amritapuri, Kollam 690525, India*
[7]*Department of Biotechnology, Faculty of Science, Bartin University, Bartin 74110, Türkiye*

Corresponding Author: ✉r.shashanka@gat.ac.in

Received: December 8, 2025; Revised: February 4, 2026; Published: February 23, 2026

Abstract

Dopamine (DA) is a vital neurotransmitter used in clinical diagnostics and neurochemical studies. In this article, a robust, accurate, and highly sensitive method for determining DA using a duplex stainless steel (DSS)-modified carbon paste electrode (MCPE) and cyclic voltammetry is reported. To improve the sensitivity of the DSS-MCPE, the electrode was polymerized via 10 potential cycles using asparagine, a non-essential amino acid, thereby forming poly(asparagine) on the electrode surface. This polymerized electrode surface acts as a selective barrier to DA and enables the DSS-MCPE to detect DA accurately, even in the presence of interfering molecules such as ascorbic and uric acids, which have overlapping oxidation potentials. Compared with the bare carbon paste electrode (BCPE) and DSS-MCPE, poly(asp)-DSS-MCPE exhibits excellent electrochemical behaviour, a higher oxidation peak current, and improved electron transfer kinetics. The effects of variations in scan rate, pH, and DA concentration on the electrocatalytic behaviour of poly(asp)-DSS-MCPE were investigated. Also, the electrode active surface area was calculated, and the limit of detection, limit of quantification, and number of electrons and protons involved in electro-chemical reactions were determined. The ease of fabrication, cost-effectiveness, and robust

performance of poly(asp)-DSS-MCPE make it a promising electrocatalyst for detecting DA and other bioactive molecules, without interference from interfering molecules.

Keywords
Catecholamine; voltametric determination; mechanical alloying, modified electrode, asparagine.

Introduction

Dopamine (DA) is an essential neurotransmitter that plays important roles in several physiological and neurological processes, including motor control, mood regulation, cognition, and endocrine signalling [1]. Its irregular concentration can cause various neurodegenerative and psychiatric disorders [2]. Therefore, we need to develop sensitive, selective, and robust analytical methods for the quantitative and qualitative determination of DA to support clinical diagnostics and neuroscience research. Currently, a handful of analytical methods, such as high-performance liquid chromatography (HPLC), chemiluminescence, spectrophotometry, and capillary electrophoresis, are used to determine DA [3,4]. However, these analytical techniques require tedious sample preparation, sophisticated instruments, and expensive chemicals, and are sometimes less selective. Therefore, new electrochemical sensing techniques are becoming very popular due to their high sensitivity, selectivity, reproducibility, cost-effectiveness, robustness, rapid response, and potential for miniaturization for real-time monitoring [5-8]. Among all electrochemical sensing techniques, cyclic voltammetry (CV) proved to be one of the most suitable and largely used techniques for determining the redox behaviour of electroactive species like DA, uric acid, ascorbic acid, riboflavin and toxic dyes [9-13].

One of the major challenges in the electrochemical determination of DA is achieving selectivity and sensitivity in biological samples, where interfering species such as ascorbic acid and uric acid coexist with DA and often overlap with its oxidation potentials [14-16]. Therefore, we have modified the carbon paste electrode (CPE) with duplex stainless steel (DSS) powders to overcome this problem and reduce the overlapping effect, thereby achieving high accuracy and selectivity. The modified carbon paste electrodes (MCPEs) increase the active surface area, act as a selective barrier, enhance electron mobility, and provide high-selectivity interaction sites for DA, thereby improving their performance. The fabricated bare carbon paste electrode (BCPE) and DSS-MCPE are composed of graphite powder and a silicone oil, which are extremely inexpensive, easy to prepare, and depict a wide potential window. Furthermore, the properties of DSS-MCPE were improved by polymerizing the electrode with asparagine, an essential amino acid, for 10 cycles using cyclic voltammetry (CV) [17]. This polymerization of DSS-MCPE further increases selectivity, electron mobility, surface area, reaction sites, sensitivity, and stability. The polymer layer on the electrode acts as a molecular sieve and allows a particular-sized and shaped ion to interact and thereby increases the selectivity of the electrode. It also reduces the oxidation overpotential, increases the peak separation, mechanical stability, reproducibility, binding affinity, and anti-fouling nature of the DSS-MCPE. Therefore, the fabricated poly(asp)-DSS-MCPE could be a promising candidate for detecting various electroactive species, such as DA.

Arpitha *et al*. electropolymerized tavaborole drug on CPE for 20 cycles over a potential range of -0.4 to 1.2 V *vs*. Ag/AgCl with a scan rate of 0.05 V/s at a pH 7.4 [18]. The MCPE showed a low heterogeneous constant of 50 mV/s toward the DA, confirming DA absorption on the MCPE. Electrochemical reactions involved an equal number of protons and electrons in detecting DA with a limit of detection (LOD) of 5.28 µM [18]. Choukairi *et al*. [19] fabricated β-cyclodextrin MCPE to determine DA with a cyclic potential range of -0.15 to 0.15 V *vs*. Ag/AgCl at pH 6. They have

successfully recovered 98 to 103.2 % of DA, and the fabricated MCPE has shown 4.8-fold higher current density than BCPE [19]. Nagles *et al.* [20], Widyaningrum *et al.* [21], Shashikumara *et al*. [22] and Varmazyar *et al*. [23] fabricated lanthanum oxide (III), ferrocene, poly(amido black), and gold nanoparticles on multi-walled carbon nanotubes (MWCNT) MCPEs, respectively, to determine DA. They have all reported excellent sensitivity, selectivity, and stability of the fabricated MCPEs.

In this article, we prepared poly(asparagine)-modified duplex stainless steel by electro-polymerizing 1 mM asparagine in phosphate-buffered saline (PBS) at pH 6.5 with a cyclic potential window of -1.0 to +1.5 V *vs*. Ag/AgCl for 10 cycles. We reported that polymerization of asparagine on the DSS-MCPE surface significantly increases surface area, conductivity, and selectivity due to strong interactions between the polymer's -NH_2 and -COOH groups and catechol.

The dual-phase (austenite and ferrite) structure of DSS imparts excellent mechanical strength, corrosion resistance, and high thermal stability compared to conventional austenitic or ferritic stainless steels [24]. In addition to their widespread structural and industrial applications, DSS powders are now used as electrocatalysts in various electrochemical sensing applications [25]. This research area remained underexplored, and we were the first to report the electrochemical sensing properties of DSS powders [26,27]. The presence of alloying elements such as chromium, nickel, and iron in DSS provides potential redox-active sites that facilitate electron transfer. The high corrosion resistance of DSS ensures long-term stability in aqueous environments, making it an attractive candidate for electrode modification [28,29]. In this article, we used the ball-milling technique to prepare DSS powders after milling for 20 hours in a toluene atmosphere, and then used them as a modifier for CPE to detect DA. This ball-milling technique is widely used to refine the microstructure of DSS. This process results in the production of nanocrystalline DSS structures with improved surface area and defect density. This further increases the electrocatalytic properties of DSS powder by exhibiting a low LOD and an anti-interference effect.

This article not only reports novel electrochemical sensing applications of DSS powders but also highlights the role of ball milling in tailoring the materials' properties to enhance electrocatalytic performance.

The fabricated DSS-MCPE, and poly(asp)-DSS-MCPE combines the benefits of ball milling, dual-phase microstructure of DSS, electrochemical sensing contributions from individual elements (Fe, Cr, and Ni) in DSS, polymerization of asparagine amino acid on the electrode surface and makes the electrodes highly sensitive, selective, stable, reproducible, and anti-fouling to detect neurotrans-mitter like DA. This research could open a new path for integrating advanced alloy materials, such as DSS and high-entropy alloys, into electrochemical sensor technologies and potentially enable biomedical and environmental sensing applications.

Experimental

The CHI-6038E electrochemical workstation, purchased in the USA, was used to investigate the electrocatalytic application of the fabricated poly(asp)-DSS-MCPE for DA detection. A three-electrode cell was used with the working, counter, and reference electrodes. The working electrode was the fabricated poly(asp)-DSS-MCPE; the counter electrode was a platinum wire; and the reference electrode was an Ag/AgCl electrode in saturated KCl. The X-ray diffraction (XRD) study was performed in PANalytical Xpert Pro XRD. Analytical grade DA, asparagine, sodium dihydrogen ortho phosphate (NaH_2PO_4), disodium hydrogen phosphate (Na_2HPO_4), silicon oil, and graphite powders were procured from Nanografi, Turkey. The standard solution of DA and a 0.1 M phosphate-buffered saline (PBS) solution were prepared in double-distilled water.

Preparation of duplex stainless steel powders

DSS powders were synthesized by ball milling the elemental iron, chromium, and nickel powders for 20 hours using a Retsch PM 100 planetary ball mill. All elemental powders were purchased from Nanografi, Turkey. The milling was carried out in toluene to prevent oxidation, and the optimized milling parameters were discussed by Shashanka *et al*. [30,31]. Every 30 minutes of milling, a 30-minute break was taken to cool the jar and prevent phase transformation in the DSS.

Fabrication of electrodes (bare carbon paste, duplex stainless steel-modified carbon paste, and poly(asp)- duplex stainless steel-modified carbon paste)

The bare CPE (BCPE) was prepared by hand-mixing graphite powder and silicone oil at a 70:30 ratio for 30 minutes using a mortar and pestle [32]. Similarly, DSS-MCPE was prepared by hand-mixing the bare CPE with DSS powder for 30 minutes. This modification of BCPE with DSS improves the electrocatalytic properties of the electrode. For further improvement of electrocatalytic properties, DSS-MCPE was electropolymerized by dissolving 1mM asparagine amino acid in a PBS solution of pH 6.5 [33] and running 10 potential cycles within the potential window of -1.0 to +1.5 V *vs.* Ag/AgCl. This caused a slight increase in the polymer oxidation current with increasing cycle number, confirming the continuous growth of poly(asparagine) on the surface of DSS-MCPE (Figure 1). When electro-polymerization begins, asparagine undergoes oxidation, generating intermediate radicals that deposit on the surface of DSS-MCPE, leading to the formation of a conductive poly(asp) layer. The polymer formed at the electrode surface increases the surface area, sensitivity, reactive sites, functional groups, and selectivity of the poly(asp)-DSS-MCPE. The formation of functional groups increases charge-transfer kinetics [34,35] and provides excellent interaction sites for DA through hydrogen bonding and electrostatic interactions.

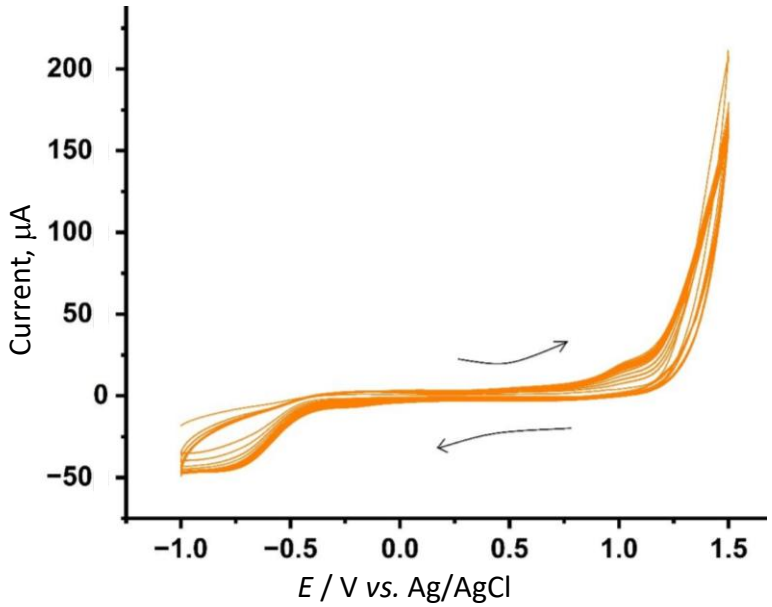

Figure 1. *Electropolymerization of 1 mM asparagine in 0.1 M PBS, pH 6.5, on DSS-MCPE by running 10 potential cycles between -1.0 and +1.5 V*

Determination of dopamine

The fabricated BCPE, DSS-MCPE, and poly(asp)-DSS-MCPE were immersed in the supporting electrolyte PBS (0.1 M) containing the analyte DA (20 to 200 μM), and cyclic voltammograms (CVs) were recorded in separate experiments. The principle of electrochemical determination of DA by poly(asp)-DSS-MCPE is graphically shown in Figure 2.

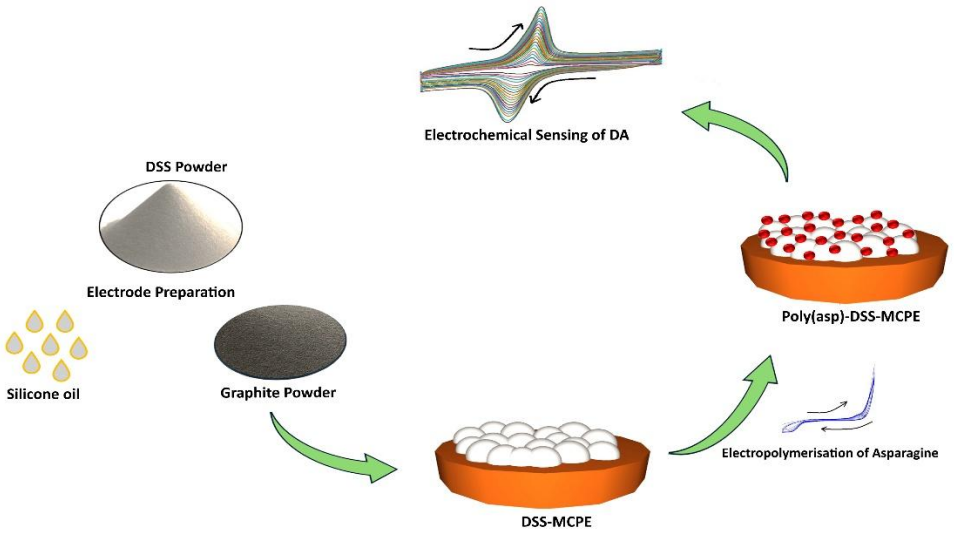

***Figure 2**. Graphical representation of electrochemical determination of DA by poly(asp)-DSS-MCPE*

Results and discussion

X-ray diffraction study of mechanically alloyed duplex stainless steel powders

The XRD pattern of the DSS powders prepared by ball milling is shown in Figure 3. The XRD confirms the substantial microstructural evolution with the formation of both austenite (γ-Fe) and ferrite (α-Fe) phases [36]. The prominent diffraction peak at approximately $2\theta \approx 44.5°$ corresponds to the (110) planes of a body-cantered cubic (BCC) α-Fe phase. On the other hand, we can observe weak and broadened peaks around 51, 60 and 74°, suggesting the presence of a face-cantered cubic (FCC) γ-Fe phase. These broad and narrow intensity diffraction peaks also appeared due to the formation of secondary or intermetallic phases resulting from high-energy milling of elemental Fe, Cr, and Ni powders [37].

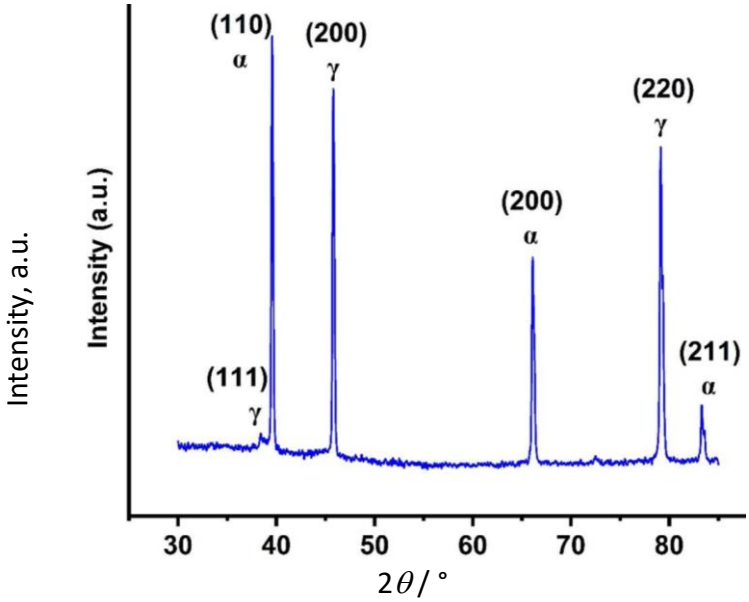

***Figure 3**. XRD pattern of mechanically alloyed DSS powder for 20 hours*

The observed diffraction peak broadening indicates the complete refinement in the microstructure forming the nanocrystallite materials, and also due to the microstrain formed because of the interaction of ball-jar-powder with maximum intensity [38]. Furthermore, the increased background intensity in the range of 2 θ angles of 70 to 90° is due to the partial amorphization and an

increased density of defects like dislocations and grain boundaries during ball milling. The XRD pattern shows no impurity peaks, confirming successful alloying of the constituent metals into homogeneous DSS powders. The overall XRD pattern confirms the formation of a nanocrystalline duplex stainless steel with a dominant ferrite phase and traces of retained austenite.

Electrochemical properties of fabricated electrodes

The electrochemical behaviour of BCPE, DSS-MCPE, and poly(asp)-DSS-MCPE was investigated using the CV technique. Figure 4 depicts the cyclic voltammograms recorded for these three electrodes in a separate set of experiments in 0.1M PBS, pH 6.5, at a scan rate of 0.1 V s^{-1} with a potential sweep from -1.0 V to 0.0 V *vs*. Ag/AgCl. The CV profile of the BCPE (blue curve) shows a relatively broad, poorly defined redox response with a low peak oxidation current (I_{pa}), indicating slow electron-transfer kinetics due to a smaller electrode surface area and fewer reaction sites. The reduced I_{pa} is also attributed to the low conductivity of the BCPE, which lacks modifiers to increase reactive sites.

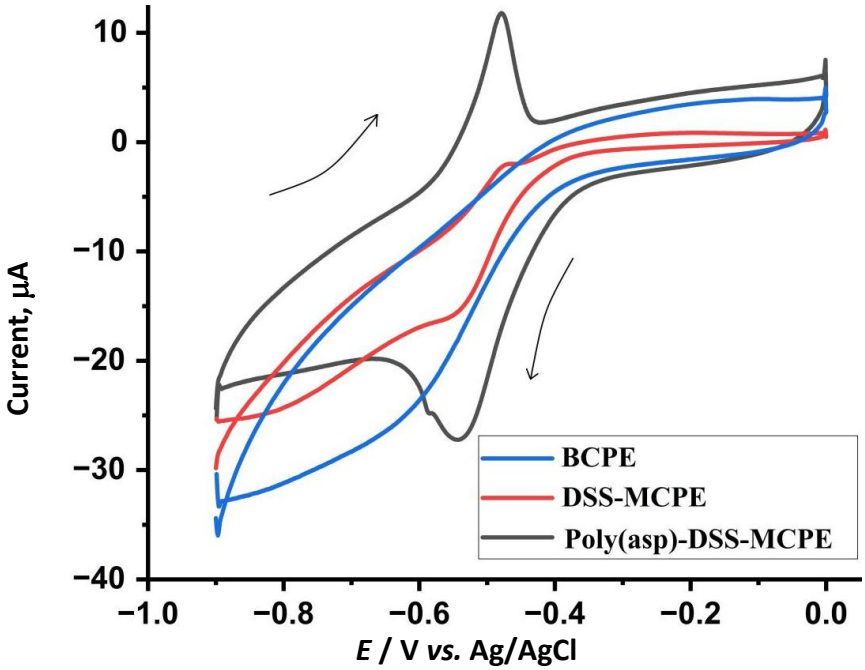

***Figure 4**. CV curves recorded individually for denoted electrodes in 0.1 M PBS, pH 6.5, containing 0.1 mM DA, at a scan rate of 0.1 V s^{-1} with potential sweep from -1.0 to 0.0 V vs. Ag/AgCl*

On the other hand, the DSS-MCPE (red curve) shows a significant increase in I_{pa} due to a relative increase in the electrode's active surface area and reaction sites, as well as faster electron-transfer kinetics. The modification also increases the electrode's conductivity by improving analyte-electrode surface interactions, thereby increasing electron mobility [39,40]. Another reason for increased I_{pa} is the presence of elements like iron, chromium, nickel, and molybdenum in DSS powders. These elements collectively enable multiple oxidation states, enhancing redox reactions and charge-transfer kinetics. In addition, the dispersed modifier, duplex stainless-steel powders, improves surface roughness and electroactive surface area, thereby providing a better platform for electron transport pathways compared to BCPE. Similarly, poly(asp)-DSS-MCPE (black curve) showed the highest I_{pa} among the BCPE, DSS-MCPE, and poly(asp)- DSS-MCPE. This polymerized DSS-MCPE with asparagine exhibits sharp, well-defined redox peaks, indicating excellent electrocatalytic properties. The main advantages of polymerizing the MCPE are the increased interaction of the functional groups like -NH_2 and -COOH present in the asparagine with the analyte DA and induce the surface-confined redox reactions. The polymerization of asparagine on the DSS-MCPE also improves the

electrode's porosity, surface area, and hydrophilic nature, along with strong adhesion. The combined effects of polymerization and electrode modification decrease the peak-to-peak separation in poly(asp)-DSS-MCPE, leading to a faster electron transfer rate and improved electrochemical reversibility compared with BCPE and DSS-MCPE.

As was discussed earlier, the electrode surface area plays an important role in the analyte's redox behaviour, and can be determined by the Randles-Ševčik Equation (1) [41-44];

$$i_p = 2.69\times10^5 n^{3/2} A D^{1/2} C v^{1/2} \quad (1)$$

where i_p / A is peak current, n is the number of electrons involved in the redox reaction, A / cm^2 is the surface area of the electrode, D / cm^2 s^{-1} is the diffusion coefficient, C mol cm^{-3} is the concentration, and v / V s^{1} is the scan rate.

The calculated active surface areas of poly(asp)-DSS-MCPE, DSS-MCPE, and BCPE are found to be 0.216, 0.067 and 0.009 cm^{2,} respectively. The increased electrode surface areas of DSS-MCPE and poly(asp)-DSS-MCPE, compared with BCPE, are responsible for the higher peak currents, as discussed earlier. This confirms that increasing the electrode's active surface area increases the redox peak currents.

Influence of pH of phosphate buffer saline electrolyte solution

To enrich the electrochemical sensor working specifications of the electrode poly(asp)-DSS--MCPE, the effect of solution pH on the redox reaction of DA was examined by changing the pH of the PBS electrolyte. Figure 5(a) displays the curves of CV for 1.0 mM DA in PBS electrolyte at a range of pH from 5.5 to 8.0 at the scan rate of 0.1 V s^{-1} at poly(asp)-DSS-MCPE.

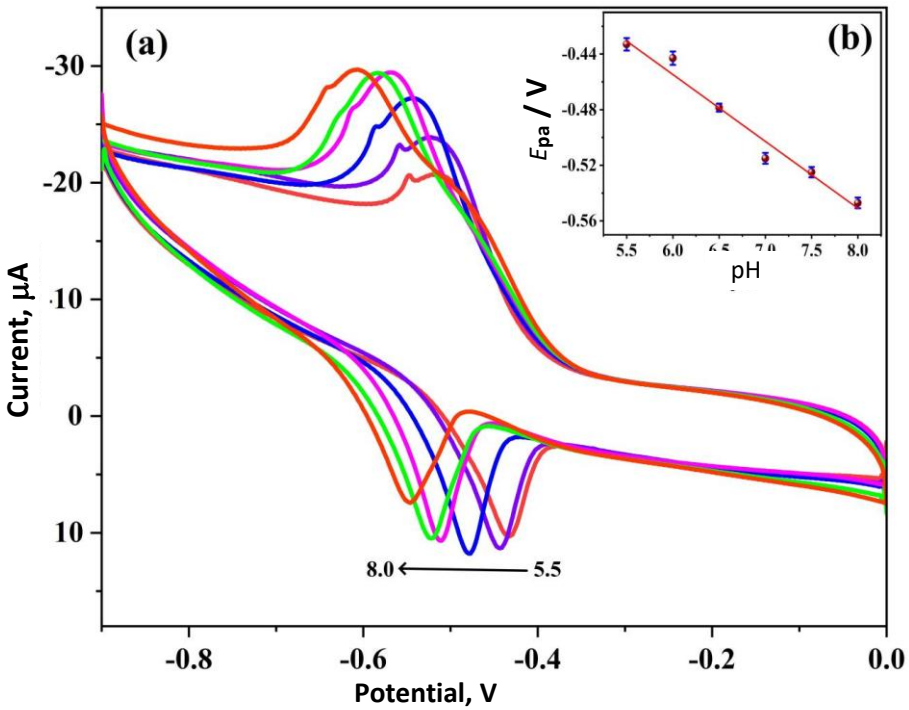

Figure 5. *(a) CVs for 0.1 mM DA in 0.1 M PBS of altered pH values (5.5 to 8.0) at the scan rate of 0.1 V s^{-1} at poly(asp)-DSS-MCPE, and (b) plot of oxidation potential (E_{pa}) vs. pH*

As the pH of PBS electrolyte was increased, both redox peak potentials of DA were decreased (shifted towards the negative value ranging between -0.4 to -0.6 V), and the oxidation peak currents of DA augmented from pH 5.5 to 6.5, and afterward oxidation peak currents dropped from pH 6.5 to 8.0, as shown in Figure 5(a). These results illustrate that the redox reaction of DA at poly(asp)--DSS-MCPE depends on the number of proton-electron transfers [45].

The most sensitive electrochemical oxidation response of DA at pH 6.5 in PBS on poly(asp)-DSS--MCPE is most likely due to the composite interface formed by several factors, such as electrostatic interactions, ionization state, ideal surface charge, and electrochemical (redox) properties. Thus, pH 6.5 was selected as the optimal electrolyte pH for all subsequent electrochemical investigations of DA. The connection between the pH of PBS and oxidation potential displays a decent linear relation (Figure 5b), and the resulting linear regression equivalence is presented by Equation (2):

E_{pa} = -0.16586 - 0.04813 pH (R^2 = 0.972) (2)

The slope of -0.048 V pH^{-1} conforms to Nernst's relation and signifies the transmission of the same number of protons and electrons during the electrochemical reaction of DA. The value of the number of protons transported was interpreted by employing the following Nernst's equation [46]:

$$\frac{dE_{pa}}{d\ pH} = \frac{-2.3\ mRT}{nF} \quad (3)$$

In this relation, dE_{pa} / d pH signifies the slope of the E_{pa} *vs*. pH plot, m signifies the number of protons transferred, n signifies the number of electrons transferred, and *T*, *R* and *F* are standard terms. The calculated value of the number of transferred protons in the redox reaction of DA was 1.625 (≈2) on poly(asp)-DSS-MCPE. The possible electrochemical reaction mechanism of DA at the surface of the modified electrode is shown in Scheme 1.

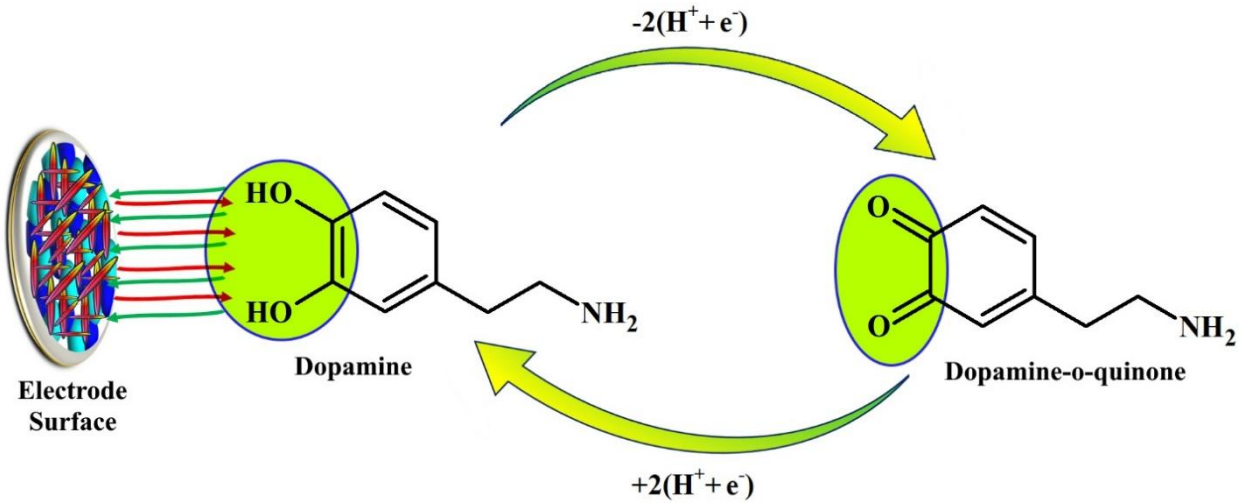

Scheme 1*: Possible electrochemical reaction mechanism of DA at the modified electrode*

Influence of scan rate

The effect of the scan rate on the redox reaction (potential and current) of 0.1 mM DA at poly(asp)--DSS-MCPE was studied in 0.1 M PBS, pH 6.5, by varying the scan rate from 0.05 to 0.50V s^{-1}. The corresponding CV curves are shown in Figure 6(a), indicating that as the scan rate increases, both the anodic and cathodic peak currents of DA increase concurrently. Also, the oxidation peak potential of DA shifts to more negative values, whereas the reduction peak potential shifts to less negative values. These outcomes indicate that the scan rate may influence the redox reaction of DA.

This effect is strongly associated with how DA cooperates with the poly(asp)-DSS-MCPE surface, either through adsorption reaction kinetics or diffusion reaction kinetics, and this is validated based on the log I_p *vs*. log ν, and I_p *vs*. ν relationships, depicted in Figures 6 (b) and 6 (c), respectively.

These graphs display a good linear association, and the subsequent linear regression Equations (4) and (5) are:

log I_{pa} = 2.265 + 1.122 log ν (R^2 = 0.997) (4)

log I_{pa} = 1.494 + 166.56 log ν (R^2 = 0.999) (5)

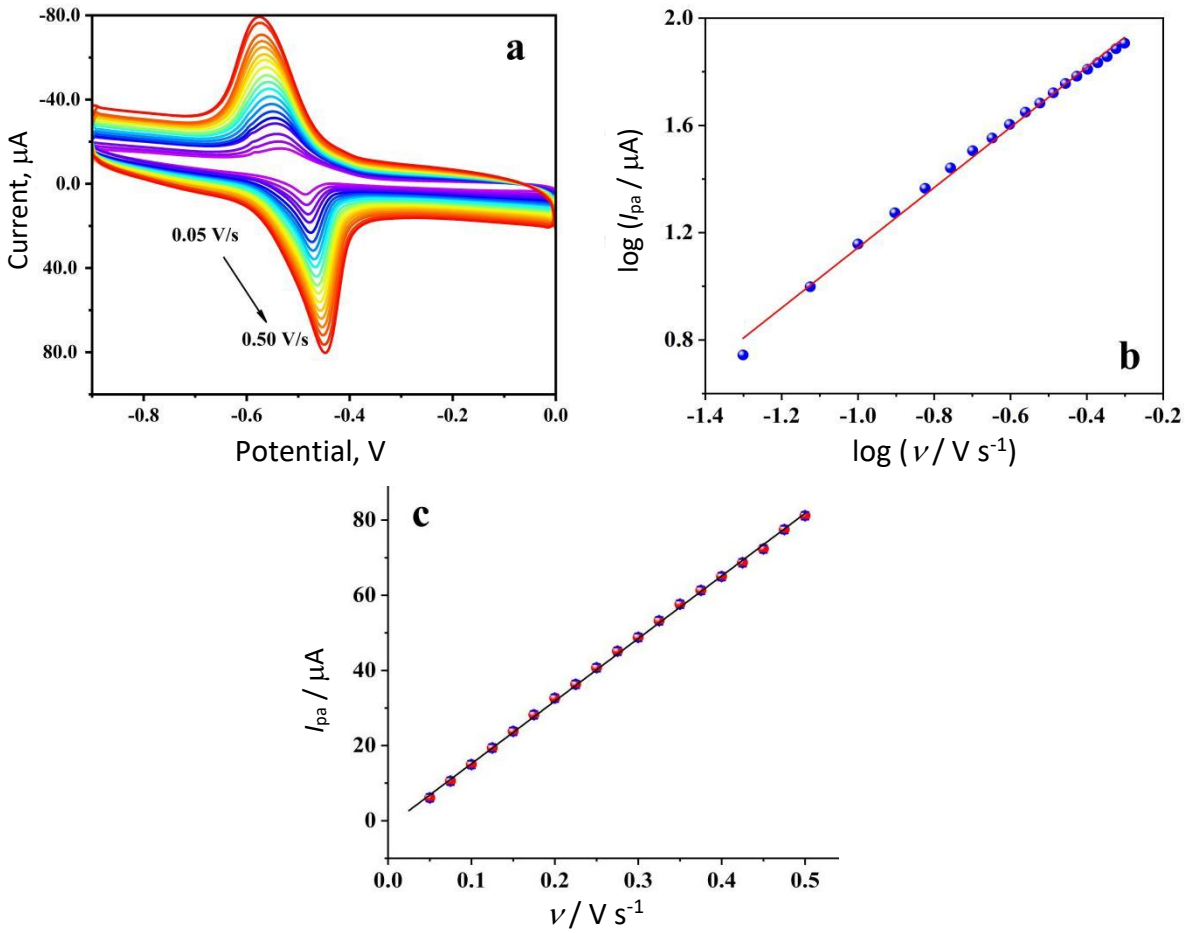

Figure 6. *(a) CV curves for 0.1 mM DA in 0.1 M PBS, pH 6.5, at scan rates (0.05 to 0.50 V s^{-1}) on poly(asp)-DSS-MCPE, (b) plot of log* I_{pa} *vs. log* ν*, (c) plot of* I_{pa} *vs.* ν

Here, the slope of 1.122 is close to the thermodynamic merit of 1.0, and the R^2 value of 0.999 is close to 1.0, indicating that the redox reaction of DA in PBS of pH 6.5 at poly(asp)-DSS-MCPE surface thoroughly obeys the adsorption-controlled kinetics [47].

Electrochemical oxidation behaviour of dopamine at different concentrations

The effect of DA concentration on the oxidation peak currents at poly(asp)-DSS-MCPE in PBS of pH 6.5 is presented in Figure 7. Figure 7(a) shows CV curves at different concentrations of DA ranging from 20 to 200 µM. From these CV curves, one can observe a clean reduction and oxidation peaks corresponding to the reversible two-electron, two-proton redox reaction of DA. As DA concentration increases from 20 to 200 µM, the oxidation peak current increases linearly in proportion to the reduction peak current. At the same time, the redox peak potentials remain almost constant, which confirms that the electrochemical redox reactions are reversible and surface-controlled within this concentration range. This linear increase in I_{pa} across different concentrations of DA indicates the excellent sensitivity and electrocatalytic behaviour of poly(asp)-DSS-MCPE. Figure 7(b) shows the linear calibration curve and confirms the excellent quantitative detection capability of poly(asp)-DSS--MCPE across a broad concentration range from 20 to 200 µM. The calibration curve is a straight line in the I_{pa} vs. DA concentration plot, with small error bars (from a minimum of 5 trials), confirming the precision and repeatability of the fabricated electrode.

Equations (6) and (7) were used to calculate the LOD and LOQ of DA at poly(asp)-DSS-MCPE, which were found to be 0.074 µM and 0.249 µM, respectively.

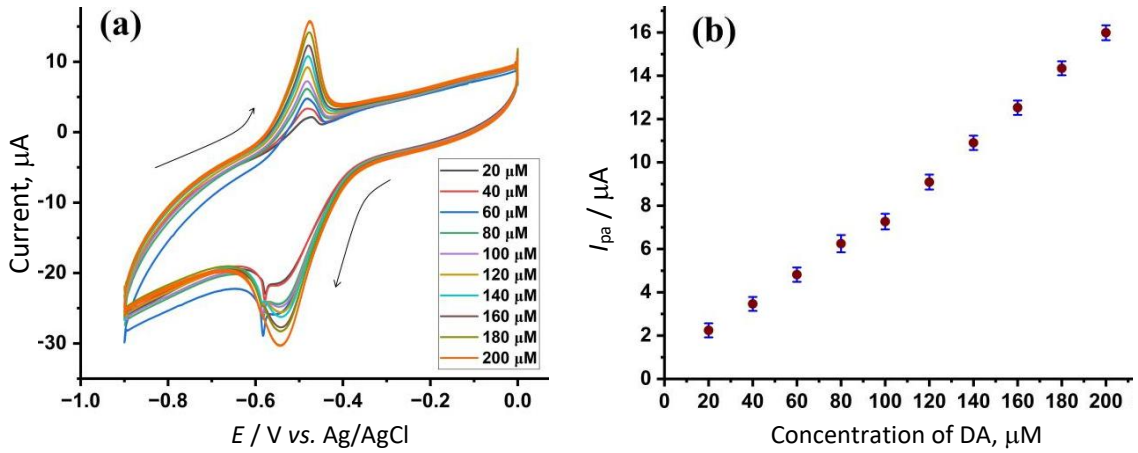

Figure 7. *(a) CV curves of DA (20 to 200 µM) in 0.1 M PBS, pH 6.5, at poly(asp)-DSS-MCPE, (b) calibration plot for DA (plot of I_{pa} vs. DA concentration)*

$$\text{LOD}=\frac{3\times\text{Standard deviation of blank}}{\text{Slope of } I_{pa} \text{ versus concentration of DA}} \quad (6)$$

$$\text{LOQ}=\frac{10\times\text{Standard deviation of blank}}{\text{Slope of } I_{pa} \text{ versus concentration of DA}} \quad (7)$$

Effect of interference ions on the electrochemical oxidation of dopamine

It is quite a challenge to determine DA in real biological fluid samples, such as blood, where DA coexists with other electroactive molecules, including uric acid (UA), ascorbic acid (AA), glucose, and ions such as Na^+, K^+, Ca^{2+}, Mg^{2+}, and Cl^-. All these electroactive species undergo electrochemical redox reactions in almost the same potential windows. In other words, these species may interfere with the redox potential of DA. As a result, it is very difficult to determine accurately in the real samples. Therefore, we must use a modifier to resolve the potential window of redox reactions. To understand the selectivity of the poly(aps)-DSS-MCPE, interference, some studies were conducted using AA, UA, Na^+, K^+, Mg^{2+}, Ca^{2+}, Cl^-, and glucose. Concentration of each interfering species was 0.1 mM, which was mixed with a known and fixed concentration of DA of 0.1 mM, and their respective I_{pa} are reported to investigate the selectivity of the poly(aps)-DSS-MCPE. Figure 8 shows that during the CV investigations, the interfering ions do not affect the I_{pa} of DA significantly, and therefore the presence of these electroactive species has no appreciable effect on the fabricated poly(aps)-DSS-MCPE.

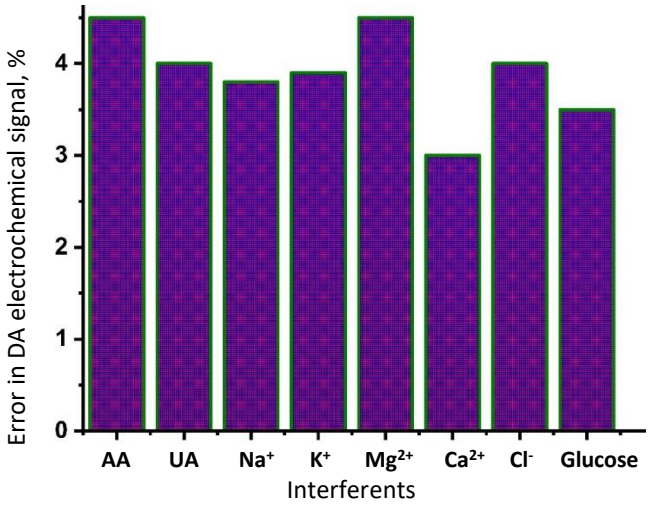

Figure 8*. Signal errors of 0.1 mM DA in 0.1 M PBS, pH 6.5 at poly(aps)-DSS-MCPE caused by the presence of 0.1 mM of denoted interferents*

The oxidation peak current of DA varied by less than ±5 % in the presence of ions and biomolecules such as AA, glucose, and UA. This demonstrated that the fabricated poly(asp)-DSS-MCPE exhibited excellent selectivity for DA in the presence of various analytes. This selectivity nature is imparted by the asparagine polymer, which was polymerized on DSS-MCPE. This polymer deposited acts as a selective barrier that can allow specific species to diffuse and interact with the electrode, and the functional groups like -NH_2 and -COOH present on the polymer and interact specifically with the catecholamines like DA via hydrogen bonding and π-π interactions.

Analysis of stability, reproducibility, and repeatability of poly(asp)-duplex stainless steel-modified carbon paste electrode

In the practical and real-world sensor applications of poly(asp)-DSS-MCPE, it is crucial to investigate stability, reproducibility, and repeatability of the fabricated electrode. These parameters ensure that the fabricated electrode performs consistently over time, across different fabrication processes, and within repeated trials.

To investigate the stability of the fabricated poly(asp)-DSS-MCPE, the electrode was stored for 3 weeks, and the CV response to 0.1 mM DA was recorded every 3 days. No significant variation (less than 5 %) in the I_{pa} of DA was observed over the 3-week period. Similarly, no change in the anodic peak potential indicates the stable redox kinetics. This excellent stability of poly(asp)-DSS-MCPE is due to the strong adhesion of poly(asparagine) to the DSS-MCPE matrix and to its chemical resistance under physiological pH conditions. Reproducibility of the poly(asp)-DSS-MCPE was investigated by electrochemically oxidizing 0.1 mM DA for 5 different times. Each time, a fresh poly(asp)-DSS-MCPE was used to determine DA, and I_{pa} value recorded in each cycle is reported. A relative standard deviation (RSD) of I_{pa} less than 4.5 % across 5 cycles indicates that the fabricated electrode exhibits high reproducibility [48]. The repeatability of the poly(aps)-DSS-MCPE was determined by measuring the CV response of DA 10 times under the same conditions, without changing the electrode. After every CV response, the poly(aps)-DSS-MCPE was rinsed with distilled water to get an accurate response. A very slight variation in the I_{pa} value across cycles was observed, with an RSD of less than 5 %. This indicates that the fabricated poly(aps)-DSS-MCPE showed significant repeatability with an excellent anti-fouling of the electrode during the CV response.

Simultaneous electrochemical determination of dopamine and riboflavin using poly(asp)-duplex stainless steel-modified carbon paste electrode

The linear sweep voltammetric (LSV) responses of DA and riboflavin (RF) analyte mixtures were investigated at BCPE and poly(asp)-DSS-MCPE in 0.1M PBS of pH 6.5, and the results are shown in Figure 9. BCPE exhibits a small, poorly defined oxidation peak, indicating poor electrocatalytic activity for simultaneously determining DA and RF due to its limited electron-transfer kinetics. On the other hand, the poly(asp)-DSS-MCPE exhibited two distinct, well-defined oxidation peaks for DA and RF, respectively. The first electrooxidation peak was observed at approximately -0.58 V, corresponding to the oxidation of DA, whereas the second oxidation peak appeared around +0.02 V, attributed to the oxidation of RF. There is a significant increase in the I_{pa} at poly(asp)-DSS-MCPE compared to BCPE when DA and RF are determined simultaneously. The increased current response at poly(asp)-DSS-MCPE is at least 5-fold higher than that of BCPE. This confirms that the poly(asp)-DSS-MCPE not only increased the current response but also resolved the anodic peaks of both DA and RF. This successful resolution of two well-separated peaks demonstrated the feasibility of simultaneously detecting DA and RF without mutual interference.

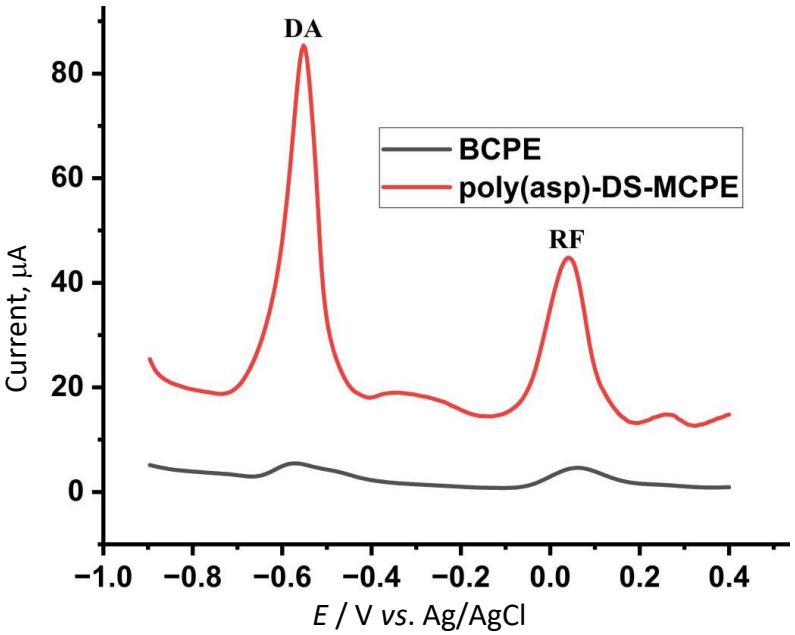

Figure 9*. LSV responses of 0.1 mM DA and 0.1 mM RF mixture in 0.1 M PBS, pH 6.5, at BCPE and poly(asp)-DSS-MCPE*

Conclusion

The ball-milled DSS powders exhibited a refined nanocrystalline dual-phase structure with a dominant α-Fe (BCC) phase and a minor γ-Fe (FCC) contribution, providing more redox-active sites and enhanced electron-transfer capability. Subsequent polymerization of asparagine for 10 potential cycles on the DSS-MCPE surface significantly increased surface area, conductivity, and selectivity, owing to strong interactions between the polymer's -NH_2 and -COOH groups and the catechol structure of DA. The poly(asp)-DSS-MCPE exhibited nearly 10-fold and 5-fold higher anodic peak current compared to BCPE and DSS-MCPE, respectively. The LOD and LOQ were calculated to be 0.074 and 0.249 µM, respectively, confirming the high detection capability of the poly(asp)-DSS-MCPE. Kinetic studies confirmed an adsorption-controlled, surface-confined electrochemical process. The poly(asp)-DSS-MCPE exhibited excellent selectivity for DA, with <±5 % current variation in the presence of common interfering species, and demonstrated strong stability, reproducibility, and antifouling behaviour (RSD < 5 %) over three weeks. The sensor successfully resolved well-separated oxidation peaks for dopamine (-0.58 V) and riboflavin (+0.02 V), enabling their simultaneous detection. Overall, the poly(asp)-DSS-MCPE is a robust, cost-effective, and reproducible platform with significant potential for advanced electrochemical sensing applications.

Conflict of interests: *The authors declare no conflict of interest.*

References

[1] S. Vishwanathan M. B. E. K. Swamy, K. A. Vishnumurthy, Iron Oxide Modified Carbon Paste Electrode Sensor for Guanine and Dopamine: A Voltammetric Technique, *Analytical and Bioanalytical Electrochemistry* **15** (6) (2023) 444-457. https://doi.org/10.22034/abec.2023.705725

[2] L. S. Manjunatha, B. E. K. Swamy, Carbon paste-glibanclamide-graphene oxide modified electrode analysis for dopamine, *Chemical Data Collections* **53** (2024) 101157. https://doi.org/10.1016/j.cdc.2024.101157

[3] S. B. Arpitha, B. E. K. Swamy, Synthesis and electrochemical performances of CuO/MgO nanocomposite as a sensing platform for dopamine, *Microchemical Journal* **206** (2024) 111584. https://doi.org/10.1016/j.microc.2024.111584
[4] B. Kanthappa, J. G. Manjunatha, Electrochemical Detection and Quantification of Anti-inflammatory Drug Diclofenac with the Presence of Dopamine Using Sensitive Poly (l-Methionine) Modified Carbon Paste Sensor, *Topics in Catalysis* **69** (2026)134-147. https://doi.org/10.1007/s11244-025-02110-2
[5] B. Kanthappa, J. G. Manjunatha, S. A. Aldossari, C. Raril, Electrochemical determination of uric acid in the presence of dopamine and riboflavin using a poly(resorcinol)-modified carbon nanotube sensor, *Scientific Reports* **15** (2025) 5822. https://doi.org/10.1038/s41598-025-90235-5
[6] K. P. Moulya, J. G. Manjunatha, S. A. Aldossari, S. Mohammad, N. Ataollahi, Recycled battery carbon composite sensor for the electrochemical analysis of the neurotransmitter dopamine, *Topics in Catalysis* **69** (2026) 259-271. https://doi.org/10.1007/s11244-025-02048-5
[7] M. I. Saidin, I. M. Isa, N. Hashim, M. S. Ahmad, S. N. A. M. Yazid, S. Kuppan, A. A. Bahari, Deciphering electrochemical activity of graphitic carbon nitride-zinc indium sulfide nanocomposite as a potential paraquat sensor, *Journal of Environmental Chemical Engineering* **13** (2025) 119012. https://doi.org/10.1016/j.jece.2025.119012
[8] M. I. Saidin, I. M. Isa, M.S. Rosmi, N. Hashim, M. S. Ahmad, S. N. A. M. Yazid, S. Kuppan, M. W. Yii, A. A. Bahari, Revolutionising pesticide detection: a high-sensitivity electrochemical sensor with CdS/g-C_3N_4/MWCNTs for paraquat monitoring, *International Journal of Environmental & Analytical Chemistry* **105** (2024) 3919-3933. https://doi.org/10.1080/03067319.2024.2356032
[9] S. Rajendrachari, R. S. Mahale, R. Ramkumar, J. Puneetha, G. K. Jayaprakash, H. Nagarajappa, Electrochemical analysis of L-Tyrosine sensor using ball-milled duplex stainless steel alloy powder, *Inorganic Chemistry Communications* **177** (2025) 114360. https://doi.org/10.1016/j.inoche.2025.114360
[10] S. Rajendrachari, G. R. Chalageri, R. S. Mahale, E. Altas, Y. Chapke, V. Adimule, Investigation of Electrocatalytic applications of various Advanced Nanostructured Alloys—An Overview, *Catalysts* **15** (2025) 259. https://doi.org/10.3390/catal15030259
[11] R. Ramkumar, P. Veerakumar, S. Rajendrachari, G. Dhakal, J. Yun, J.-J. Shim, W. K. Kim, Copper aerogel frameworks—Electrochemical detection of dopamine and catalytic reduction of 4-nitrophenol, *Microchemical Journal* **208** (2024) 112486. https://doi.org/10.1016/j.microc.2024.112486
[12] S. Rajendrachari, R. Vinaykumar, R. Katti, B. G. Koujalagi, G. K. Jayaprakash, R. Ramkumar, Cyclic voltammetric determination of rhodamine B dye using a Gas-Atomized duplex stainless steel Powder-Modified carbon paste electrode, *Topics in Catalysis* **69** (2026) 307-318. https://doi.org/10.1007/s11244-024-02020-9
[13] S. Rajendrachari, E. Altaş, A. Erdogan, Y. Küçük, M. S. Gök, F. Khosravi, Electrochemical determination of dopamine by poly (methyl orange) shape memory alloy modified carbon paste electrode, *Inorganic Chemistry Communications* **167** (2024) 112826. https://doi.org/10.1016/j.inoche.2024.112826
[14] M. Pirsaheb, S. Mohammadi, A. Salimi, Current advances of carbon dots based biosensors for tumor marker detection, cancer cells analysis and bioimaging, *TrAC Trends in Analytical Chemistry* **115** (2019) 83-99. https://doi.org/10.1016/j.trac.2019.04.003
[15] H. M. Stapleton, J. M. Keller, M. M. Schantz, J. R. Kucklick, S. D. Leigh, S. A. Wise, Determination of polybrominated diphenyl ethers in environmental standard reference materials, *Analytical and Bioanalytical Chemistry* **387** (2007) 2365-2379. https://doi.org/10.1007/s00216-006-1054-5

[16] M. R. A. M. Roduan, M. I. Saidin, S. M. Sidik, J. Abdullah, I. M. Isa, N. Hashim, M. S. Ahmad, S. N. A. M. Yazid, A. Ul-Hamid, A. A. Bahari, New modified mesoporous silica nanoparticles with bimetallic Ni-Zr for electroanalytical detection of dopamine, *Journal of Electrochemical Science and Engineering* **12** (2022) 463-474. https://doi.org/10.5599/jese.1200

[17] B. Coldibeli, N. S. M. Campos, C. A. R. Salamanca-Neto, J. Scremin, G. J. Mattos, G. G. Marcheafave, E. R. Sartori, Feasibility of the use of boron-doped diamond electrode coupled to electroanalytical techniques for the individual determination of pravastatin and its association with acetylsalicylic acid, *Journal of Electroanalytical Chemistry* **862** (2020) 113987. https://doi.org/10.1016/j.jelechem.2020.113987

[18] S. B. Arpitha, B. E. K. Swamy, S. C. Sharma, M. R. Sanjana, S. Varamahalakshmi, Voltammetric study of dopamine at tavaborole modified carbon paste electrode, *Sensing Technology* **2** (2024) 2305873. https://doi.org/10.1080/28361466.2024.2305873

[19] M. Choukairi, M. B. Atia, M. Achache, D. Bouchta, Voltammetric detection of dopamine using a β-cyclodextrin modified carbon paste electrode: Application to human serum, *Microchemical Journal* **214** (2025) 114035. https://doi.org/10.1016/j.microc.2025.114035

[20] E. Nagles, F. Riesco, L. Roldan-Tello, Electrochemical Determination of Dopamine with a Carbon Paste-Lanthanum (III) Oxide Micro-Composite Electrode: Effect of Cetyl Trimethyl Ammonium Bromide Surfactant on Selectivity, *Sensors* **24** (2024) 5420. https://doi.org/10.3390/s24165420

[21] B. A. Widyaningrum, N. Widianti, M. Harsiniand, A. Purwaningsih, Selective voltammetric detection of dopamine using ferrocene modified carbon paste electrode, *IOP Conference Series Earth and Environmental Science* **572** (2020) 012037. https://doi.org/10.1088/1755-1315/572/1/012037

[22] J. K. Shashikumara, B. E. K. Swamy, H. D. Madhuchandra, Poly(amido black) modified carbon paste electrode sensor for dopamine in the presence of uric acid, *Materials Science for Energy Technologies* **3** (2020) 390-396. https://doi.org/10.1016/j.mset.2020.02.004

[23] N. Varmazyar, Z. Pourghobadi, Z. Derikvand, Voltammetric determination of dopamine using Au nanoparticles decorated on Multi-walled carbon nanotubes and B-Cyclodextrin modified glassy carbon electrode, *Iranian Journal of Chemistry and Chemical Engineering* **43** (2024) 1928-1936. https://doi.org/10.30492/ijcce.2023.2005214.6090

[24] S. Amirkhanlou, M. R. Rezaei, B. Niroumand, M. R. Toroghinejad, High-strength and highly-uniform composites produced by compocasting and cold rolling processes, *Materials & Design* **32** (2011) 2085-2090. https://doi.org/10.1016/j.matdes.2010.11.046

[25] M. Zapponi, T. Pérez, C. Ramos, C. Saragovi, Prohesion and outdoors tests on corrosion products developed over painted galvanized steel sheets with and without Cr(VI) species, *Corrosion Science* **47** (2004) 923-936. https://doi.org/10.1016/j.corsci.2004.06.007

[26] R. S. Mahale, V. Rajashekar, S. Vasanth, S. P. Chikkegowda, S. Rajendrachari, V. Mahesh, Fabrication of mechanically alloyed super duplex Stainless Steel Powder-Modified Carbon Paste electrode for the determination of methylene blue by the Cyclic Voltammetry technique, *ACS Omega* **9** (2024) 10660-10670. https://doi.org/10.1021/acsomega.3c09163

[27] R. S. Mahale, S. Vasanth, S. P. Chikkegouda, S. Rajendrachari, D. Narsimhachary, N. Basavegowda, Electrochemical determination of ascorbic acid by mechanically alloyed super duplex stainless steel powders, *Metals* **13** (2023) 1430. https://doi.org/10.3390/met13081430

[28] S. Rajendrachari, Investigation of electrochemical pitting corrosion by linear sweep voltammetry: a fast and robust approach, in *Voltammetry*, N. W. Maxakato, S. S. Gwebu, G. H. Mhlongo, Eds., IntechOpen eBooks, London, UK, 2019. https://doi.org/10.5772/intechopen.80980

[29] R. Shashanka, D. Chaira, K. S. Be, Effect of Y_2O_3 nanoparticles on corrosion Study of Spark plasma sintered duplex and ferritic stainless steel samples by linear sweep voltammetric method, *Archives of Metallurgy and Materials* **63** (2018) 749-763. https://doi.org/10.24425/122401
[30] R. Shashanka, D. Chaira, Development of nano-structured duplex and ferritic stainless steels by pulverisette planetary milling followed by pressureless sintering, *Materials Characterization* **99** (2014) 220-229. https://doi.org/10.1016/j.matchar.2014.11.030
[31] R. Shashanka, D. Chaira, Optimization of milling parameters for the synthesis of nano-structured duplex and ferritic stainless steel powders by high energy planetary milling, *Powder Technology* **278** (2015) 35-45. https://doi.org/10.1016/j.powtec.2015.03.007
[32] M. Harsini, B. A. Widyaningrum, E. Fitriany, D. R. A. Paramita, A. N. Farida, A. Baktir, F. Kurniawan, S. C. W. Sakti, Electrochemical synthesis of polymelamine/gold nanoparticle modified carbon paste electrode as voltammetric sensor of dopamine, *Chinese Journal of Analytical Chemistry* **50** (2022) 100052. https://doi.org/10.1016/j.cjac.2022.100052
[33] J. R. Windmiller, J. Wang, Wearable Electrochemical Sensors and Biosensors: A review, *Electroanalysis* **25** (2012) 29-46. https://doi.org/10.1002/elan.201200349
[34] T. F. Hassen, T. Gharbi, H. Cattey, G. Herlem, Electropolymerization of some amino acids on platinum electrode, *Revista Bionatura* **8** (2023) 64. https://doi.org/10.21931/RB/2023.08.02.64
[35] A. J. Bard, L. R. Faulkner, *Electrochemical Methods: Fundamentals and Applications,* John Wiley & Sons, New York, 2004. ISBN 0-471-04372-9
[36] W. Sheng, J. Li, B. Fu, T. Dong, G. Li, S. Ma, H. Shao, Z. Niu, Study on microstructure and properties evolution of duplex stainless steel powders by high-energy ball milling, *Journal of Materials Research and Technology* **33** (2024) 2014-2022. https://doi.org/10.1016/j.jmrt.2024.09.199
[37] R. Shashanka, O. Uzun, D. Chaira, Synthesis of Nano-Structured Duplex and Ferritic Stainless Steel Powders by Dry Milling and Its Comparison with Wet Milling, *Archives of Metallurgy and Materials* **65** (2020) 5-14. https://doi.org/10.24425/amm.2019.131091
[38] R. S. Mahale, S. Vasanth, P. C. Sharath, R. Shashanka, V. Tambrallimath, A. Badari, Effect of ball to powder ratios on the phase transformation of austenite and ferrite during ball milling of SAF-2507 Super Duplex stainless steel powders, *Journal of the Institution of Engineers (India) Series D* **105** (2024) 1875-1888. https://doi.org/10.1007/s40033-023-00624-1
[39] D. Merli, A. Cutaia, I. Hallulli, A. Bonanni, G. Alberti, Molecularly imprinted Polypyrrole-Modified Screen-Printed electrode for dopamine determination, *Polymers* **16** (2024) 2528. https://doi.org/10.3390/polym16172528
[40] S. Watzele, P. Hauenstein, Y. Liang, S. Xue, J. Fichtner, B. Garlyyev, D. Scieszka, F. Claudel, F. Maillard, A.S. Bandarenka, Determination of electroactive surface area of NI-, CO-, Fe-, and Ir-Based oxide electrocatalysts, *ACS Catalysis* **9** (2019) 9222-9230. https://doi.org/10.1021/acscatal.9b02006
[41] R. H. R. Mohammed, R. Y. A. Hassan, R. Mahmoud, A. A. Farghali, M. E. M. Hassouna, Electrochemical determination of cadmium ions in biological and environmental samples using a newly developed sensing platform made of nickel tungstate-doped multi-walled carbon nanotubes, *Journal of Applied Electrochemistry* **54** (2023) 657-668. https://doi.org/10.1007/s10800-023-01976-y
[42] S. Rajendrachari, H. Arslanoglu, A. Yaras, S. M. Golabhanvi, Electrochemical Detection of Uric Acid Based on a Carbon Paste Electrode Modified with Ta_2O_5 Recovered from Ore by a Novel Method, *ACS Omega* **8** (2023) 46946-46954. https://doi.org/10.1021/acsomega.3c06749

[43] M. Javed, A. Shah, M. U. Farooq, An electroanalytical sensor for the detection of antibiotic cefoperazone sodium sulbactam sodium residue in wastewater, *RSC Advances* **15** (2025) 2011-2022. https://doi.org/10.1039/d4ra08139k
[44] P. Narasimhappa, P. C. Ramamurthy, An electrochemical approach for tryptophan detection that regulates the kynurenine pathway, *Scientific Reports* **15** (2025) 23421. https://doi.org/10.1038/s41598-025-86587-7
[45] N. S. Anuar, W. J. Basirun, Md. Shalauddin, S. Akhter, A dopamine electrochemical sensor based on a platinum-silver graphene nanocomposite modified electrode, *RSC Advances* **10** (2020) 17336-17344. https://doi.org/10.1039/c9ra11056a
[46] X. T. Peter, C.-Y. Kuo, P. Malar, M. Govindasamy, U. Rajaji, K. Yusuf, Electrochemical detection of antimalarial drug (Amodiaquine) using Dy-MOF@MWCNTs composites to prevent erythrocytic stages of plasmodium species in human bodies, *Microchemical Journal* **202** (2024) 110790. https://doi.org/10.1016/j.microc.2024.110790
[47] B. Kanthappa, J. G. Manjunatha, S. M. Osman, N. Ataollahi, Electrochemical polymerized DL-phenylalanine modified carbon nanotube sensor for the selective and sensitive determination of caffeic acid with riboflavin, *Scientific Reports* **14** (2024) 30950. https://doi.org/10.1038/s41598-024-82011-8
[48] Y. M. Ahmed, M. A. Eldin, A. Galal, N. F. Atta, Electrochemical sensor for simultaneous determination of trifluoperazine and dopamine in human serum based on graphene oxide-carbon nanotubes/iron-nickel nanoparticles, *RSC Advances* **13** (2023) 25209-25217. https://doi.org/10.1039/d3ra04334g